Neutron Skin Thickness of Nuclei and Effective Nucleon–Nucleon Interactions *

LIU Min(刘敏)[1,2], WANG Ning(王宁)[2], LI Zhu-Xia(李祝霞)[1,3,4**], WU Xi-Zhen(吴锡真)[1,4]

[1] *China Institute of Atomic Energy, Beijing 102413*

[2] *Institute for Theoretical Physics at the Justus-Liebig-University Giessen, D-35392, Germany*

[3] *Institute of Theoretical Physics, Chinese Academy of Sciences, Beijing 100080*

[4] *Nuclear Theory Center of National Laboratory of Heavy Ion Accelerator, Lanzhou 730000*

(Received 27 December 2005)

The Skyrme energy density functional is applied to study the ground state properties of a series of finite nuclei. The charge rms radii, neutron rms radii, and the neutron skin thickness for some nuclei are calculated and compared with the experimental data. The constraint on the effective interactions, especially, the density dependence of the isospin-dependent part of Skyrme interactions is extracted by the data of neutron skin thicknesses of ^{208}Pb and isotopes of Sn.

PACS: 21. 30. Fe, 21. 10. Gv, 21. 10. Dr

There has been considerable interest in the neutron density distribution and the thickness of neutron skin of nuclei both theoretically and experimentally.[1−4] It has been shown that the thickness of neutron skin of nuclei closely related to the density dependence of the symmetry energy and is an important observable for probing the symmetry potential of nuclear matter. There has been accumulated a few data on the neutron skin thickness of nuclei such as ^{208}Pb, the isotopes of Sn and Ca. These data provide us with a good testing ground for effective nucleon-nucleon interactions. The methods for extracting the neutron-skin thickness usually including hadron scattering, π^- elastic scattering, antiprotonic atoms, parity-violating electron scattering, the giant dipole resonance method and spin-dipole resonance method. Recently, the isospin diffusion data in heavy ion collisions are also applied to extract the neutron-skin thickness of heavy nuclei.[6] Table 1 gives a summary of the neutron-skin thickness obtained in different methods.[5,6] One can see from the table that the neutron-skin thicknesses obtained by different methods are not consistent due to the model-dependent analysis and the accuracy of the measurements . Nevertheless, one can still ask if we can learn something about the effective interaction with these experimental data? The aim of this work is to seek the constraint on the effective interactions from the present existing data of neutron-skin thicknesses.

Table 1. The data for the neutron skin thickness of Sn isotopes and ^{208}Pb.

Nuclei	(p,p)[7,8]	(p,p)[9]	GDR[11]	SDR1[12]	SDR2[5]	Antiproton[10]
^{114}Sn				≤ 0.09	0.13 ± 0.01	
^{116}Sn	0.15 ± 0.05		0.02 ± 0.12	0.12 ± 0.06	0.15 ± 0.01	0.12 ± 0.02
^{118}Sn				0.13 ± 0.06	0.18 ± 0.01	
^{120}Sn				0.18	0.21 ± 0.01	0.12 ± 0.02
^{122}Sn				0.22 ± 0.07	0.23 ± 0.01	
^{124}Sn	0.25 ± 0.05		0.21 ± 0.11	0.19 ± 0.07	0.26 ± 0.01	0.19 ± 0.02
^{208}Pb	0.14 ± 0.04	0.20 ± 0.04	0.19 ± 0.09		0.12 ± 0.07	0.15 ± 0.02

According to the Hohenberg and Kohn theorem,[13] the energy of an N-body system of interaction fermions is a unique functional of local density. In the framework of the semi-classical extended Thomas–Fermi (ETF) approach together with a Skyrme effective nuclear interaction such a functional can be derived analytically. The density functional theory can be widely used in many-body problems which provides us with a useful balance between accuracy and computation cost allowing large systems with a simple self-consistent manner. In this Letter, we apply the semi-classical expressions of the Skyrme energy density functional to study the ground state energies, the proton neutron density distributions, and neutron skin thicknesses of a series of nuclei by the restricted density variational (RDV) method.[14−16]

The binding energy of a nucleus can be expressed as the integral of energy density functional

$$E = \int \mathcal{H} d\boldsymbol{r}. \quad (1)$$

The energy density functional $\mathcal{H}$ includes the kinetic, nuclear interaction and Coulomb interaction energy parts

$$\mathcal{H} = \frac{\hbar^2}{2m}[\tau_p(\boldsymbol{r}) + \tau_n(\boldsymbol{r})] + \mathcal{H}_{\rm sky}(\boldsymbol{r}) + \mathcal{H}_{\rm coul}(\boldsymbol{r}). \quad (2)$$

For the kinetic energy part, the extended Thomas–Fermi (ETF) approach including all terms up to sec-

* Supported by the National Natural Science Foundation of China under Grant Nos 10235030 and 10235020, the Major State Basic Research Development Programme under Contract No G20000774.

** To whom correspondence should be addressed. Email: lizwux@iris.ciae.ac.cn

ond order (ETF2) and forth order (ETF4) in the spatial derivatives is adopted as in Ref. [14]. The kinetic energy densities of protons ($i = p$) and neutrons ($i = n$) with ETF2 are given by

$$\tau_i(\boldsymbol{r}) = \frac{3}{5}(3\pi^2)^{2/3}\rho_i^{5/3} + \frac{1}{36}\frac{(\nabla\rho_i)^2}{\rho_i} + \frac{1}{3}\Delta\rho_i + \frac{1}{6}\frac{\nabla\rho_i\nabla f_i + \rho_i\Delta f_i}{f_i} - \frac{1}{12}\rho_i\Big(\frac{\nabla f_i}{f_i}\Big)^2 + \frac{1}{2}\rho_i\Big(\frac{2m}{\hbar^2}\frac{W_0}{2}\frac{\nabla(\rho+\rho_i)}{f_i}\Big)^2, \quad (3)$$

where ρ_i denotes the proton or neutron density of the nucleus and $\rho = \rho_p + \rho_n$; W_0 denotes the strength of the Skyrme spin-orbit interaction; $f_i(\boldsymbol{r})$ in Eq. (3) reads

$$f_i(\boldsymbol{r}) = 1 + \frac{2m}{\hbar^2}[B_3\rho(\boldsymbol{r}) + B_4\rho_i(\boldsymbol{r})], \quad (4)$$

with $B_3 = \frac{1}{4}\Big[t_1\Big(1+\frac{x_1}{2}\Big) + t_2\Big(1+\frac{x_2}{2}\Big)\Big]$ and $B_4 = \frac{1}{4}\Big[t_2\Big(x_2+\frac{1}{2}\Big) - t_1\Big(x_1+\frac{1}{2}\Big)\Big]$. The nuclear interaction part with Skyrme interaction $\mathcal{H}_{\rm sky}$ reads

$$\begin{aligned}\mathcal{H}_{\rm sky}(\boldsymbol{r}) = {}& \frac{t_0}{2}\Big[\Big(1+\frac{1}{2}x_0\Big)\rho^2 - \Big(x_0+\frac{1}{2}\Big)(\rho_p^2+\rho_n^2)\Big] \\ & + \frac{1}{12}t_3\rho^\alpha\Big[\Big(1+\frac{1}{2}x_3\Big)\rho^2 - \Big(x_3+\frac{1}{2}\Big)(\rho_p^2+\rho_n^2)\Big] \\ & + \frac{1}{4}\Big[t_1\Big(1+\frac{1}{2}x_1\Big) + t_2\Big(1+\frac{1}{2}x_2\Big)\Big]\tau\rho \\ & + \frac{1}{4}\Big[t_2\Big(x_2+\frac{1}{2}\Big) - t_1\Big(x_1+\frac{1}{2}\Big)\Big](\tau_p\rho_p + \tau_n\rho_n) \\ & + \frac{1}{16}\Big[3t_1\Big(1+\frac{1}{2}x_1\Big) - t_2\Big(1+\frac{1}{2}x_2\Big)\Big](\nabla\rho)^2 \\ & - \frac{1}{16}\Big[3t_1\Big(x_1+\frac{1}{2}\Big) + t_2\Big(x_2+\frac{1}{2}\Big)\Big][(\nabla\rho_n)^2 + (\nabla\rho_p)^2] \\ & - \frac{W_0^2}{4}\frac{2m}{\hbar^2}\Big[\frac{\rho_p}{f_p}(2\nabla\rho_p + \nabla\rho_n)^2 + \frac{\rho_n}{f_n}(2\nabla\rho_n + \nabla\rho_p)^2\Big], \end{aligned} \quad (5)$$

where t_0, t_1, t_2, t_3, x_0, x_1, x_2, x_3, and α are the Skyrme-force parameters.[15] The last term on the right-hand side of expression (5) is the semi-classical expansions (up to the second order in $\hbar$) of spin-orbit densities. The Coulomb energy density can be written as the sum of the direct and exchange terms, the latter taken into account in the Slater approximation,

$$\mathcal{H}_{\rm Coul}(\boldsymbol{r}) = \frac{e^2}{2}\rho_p(\boldsymbol{r})\int\frac{\rho_p(\boldsymbol{r}')}{|\boldsymbol{r}-\boldsymbol{r}'|}d\boldsymbol{r}' - \frac{3e^2}{4}\Big(\frac{3}{\pi}\Big)^{1/3}(\rho_p(\boldsymbol{r}))^{4/3}. \quad (6)$$

From Eqs. (1)–(6), one can see that the total energy of a nuclear system can be expressed as a functional of proton and neutron densities [$\rho_p(\boldsymbol{r})$ and $\rho_n(\boldsymbol{r})$] under the Skyrme interaction associated with the ETF approximation.

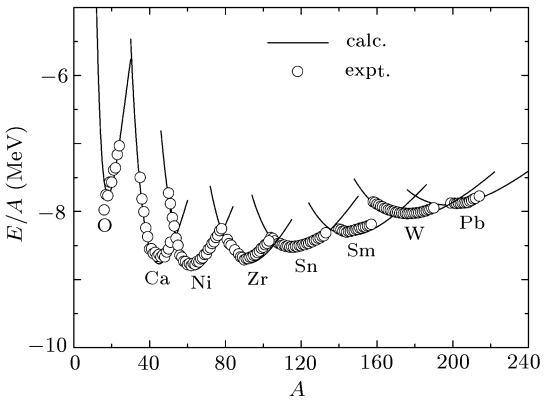

Fig. 1. The average energies per nucleon E/A for isotopes of O, Ca, Ni, Zr, Sn, Sm, W, and Pb calculated by the RDV approach (solid curves). The open circles denote the corresponding experimental data.

By minimizing the total energy of the system given by expression (1), the neutron and proton densities can be obtained. The neutron and proton density distributions are taken to be the spherical symmetric Fermi function:

$$\rho_i(\boldsymbol{r}) = \rho_{0i}\Big[1 + \exp\Big(\frac{r - R_{0i}}{a_i}\Big)\Big]^{-1}, \quad i = \{n, p\}. \quad (7)$$

Here R_{0p}, a_p R_{0n}, and a_n are the radius and diffuseness of proton and neutron density distributions, respectively. Among three quantities ρ_{0i}, R_{0i} and a_i in Eq. (7), only two of them are independent due to the conservation of total particle number.

By using optimization algorithm, one can obtain the minimal energy E_b as well as the corresponding R_{0p}, a_p, R_{0n}, a_n for the neutron and proton density distributions.

First we calculate the energies per nucleon E/A for a series of nuclei as a test of the model. Figure 1 shows the energies per nucleon for isotopes of O, Ca, Ni, Zr, Sn, Sm, W, and Pb calculated with SkM*. The experimental data are also presented in the figure for comparison. One can see that the calculation results are in good agreement with experimental data except very light nuclei with an error of about 0.5 MeV.

In Fig. 2, we show the proton and neutron density distributions for Ca, Zr, Sn, and Pb isotopes. One sees that for neutron density distributions, the central density and surface extension increase with the increasing number of neutron for given proton number Z, while for proton density distributions, the central density decreases and the surface extension increases with the number of neutron increasing. This indicates that the increased neutrons may push the protons to the surface of the nucleus due to neutron-proton interaction. The behaviour of proton and neutron density distributions founded in this work is similar with that in Ref. [17] in which the HF+BCS method was adopted. The point is that much more computation cost is saved by the method used in this work.

Figure 3 shows the neutron skin thicknesses of isotopes of ^{114}Sn, ^{116}Sn,^{118}Sn,^{120}Sn,^{122}Sn and ^{124}Sn cal-

culated with 45 Skyrme interactions, published since 1972.[18] All calculations are with ETF4. The neutron skin thicknesses calculated with ETF4 are slightly larger than those of ETF2. Corresponding experimental data[5] are also shown in this figure. One can see from the figure that neutron skin thicknesses calculated with different Skyrme interactions are largely divergent. The new data obtained by the SDR method (denoted as SDR2) are much larger than the previous data with SDR (denoted with SDR1) and with antiprotonic atom method. The data with SDR2 can be described by SKT4-5, SKO and SKI1. The characteristic feature of this group of Skyrme interactions is their symmetry energy, which belongs to the most stiff symmetry energy among 45 Skyrme interactions. While the data obtained by SDR1 and antiprotonic atom are better described by SKT1-3, SKMP, and SLy series. The symmetry energy for this group of Skyrme interactions is not so stiff as the previous group. The data for the neutron skin thickness of ^{208}Pb obtained by the antiprotonic atom can be described by SKM*, SKp, SKX, SII, SKT1-3, SKT6-9, MSK1,2 and SLy series, the group of Skyrme interactions with soft symmetry energy.

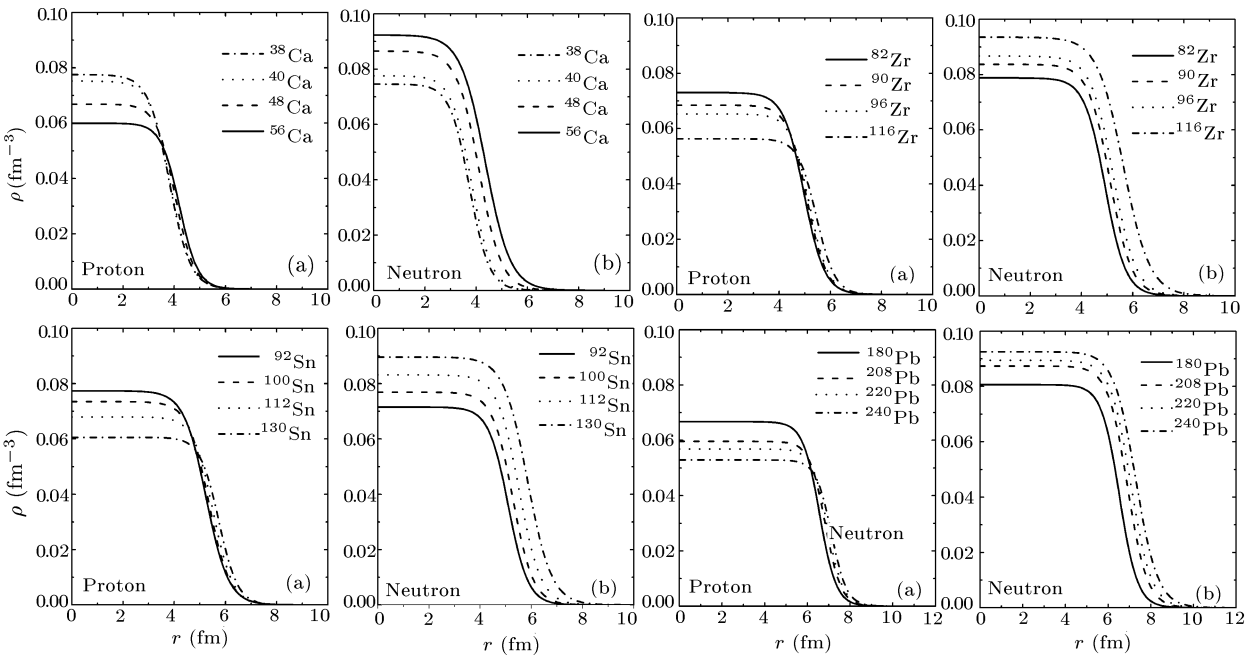

Fig. 2. The proton and neutron densities of the isotopes of Ca, Zr, Sn, and Pb, respectively.

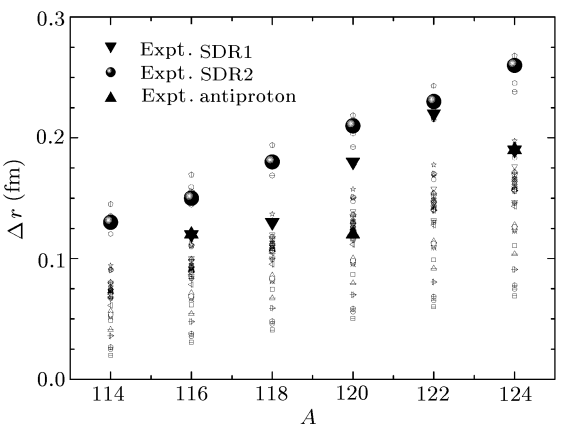

Fig. 3. The neutron skin thicknesses ($\Delta r = r_{\rm n} - r_{\rm p}$) of isotopes of ^{114}Sn, ^{116}Sn, ^{118}Sn, ^{120}Sn, ^{122}Sn, and ^{124}Sn calculated with 45 Skyrme interactions (open symbols) and the corresponding data from different experimental methods.

Now let us discuss the constraint on the density dependence of the symmetry energy from the data available till now. The equation of state (EOS) for asymmetrical nuclear matter can be given empirically as

$$e(\rho,\delta) = e(\rho,0) + e_{\rm sym}(\rho)\delta^2 + \mathcal{O}(\delta^4). \qquad (8)$$

Here $e(\rho,0)$ is the iso-scaler part, $e_{\rm sym}$ is the bulk symmetrical energies, and $\delta = (\rho_n - \rho_p)/(\rho_n + \rho_p)$ is the degree of the isospin asymmetry. Near the saturated density, $e_{\rm sym}$ can be expanded as

$$e_{\rm sym}(\rho) = e_{\rm sym}(\rho_0) + \frac{L}{3}\Big(\frac{\rho-\rho_0}{\rho_0}\Big) + \frac{K_{\rm sym}}{18}\Big(\frac{\rho-\rho_0}{\rho_0}\Big)^2 + \cdots. \qquad (9)$$

$e_{\rm sym}(\rho_0)$ is the symmetry energy coefficient, $L = 3\rho_0 \dfrac{\partial e_{\rm sym}}{\partial \rho}\Big|_{\rho=\rho_0}$ and $K_{\rm sym} = 9\rho_0^2 \dfrac{\partial^2 e_{\rm sym}}{\partial \rho^2}\Big|_{\rho=\rho_0}$ give the slope and the curvature of the symmetry energy near the saturated density, respectively. L and $K_{\rm sym}$ give the density dependence of the symmetry energy near saturated nuclear density. Figure 4 plots the neutron skin thicknesses of ^{48}Ca, ^{18}O, ^{124}Sn, ^{132}Sn and ^{208}Pb as a function of L(a) and $K_{\rm sym}$(b) calculated with all available Skyrme interactions, respectively. The calculation results with different Skyrme

interactions are largely divergent. The figure shows a tendency that the neutron skin thickness increases with the increase of L and $K_{\rm sym}$ as that given in Ref. [19]. In the figure we also indicate the data obtained by different methods. The solid line gives the data for neutron skin thicknesses obtained with SDR2, the dashed line gives those with the anti-protonic atom method and the dot-dashed line gives the results with the (p,p) method. From the data of the neutron skin thickness of ^{124}Sn obtained with the antiproton atom method, the ranges of $22 \sim 75$ MeV for L and $-261 \sim -40$ MeV for $K_{\rm sym}$ can be obtained. While the ranges of $98 \sim 161$ MeV for L and $-25 \sim 235$ MeV for $K_{\rm sym}$ are obtained from the data of neutron skin thickness of ^{124}Sn obtained with SDR2. From the data of the neutron skin thickness of ^{208}Pb with the (p,p) method we obtain the ranges of $48 \sim 95$ MeV for L and $-255 \sim -24$ MeV for $K_{\rm sym}$, while that of ^{208}Pb with the SDR2 method suggests L in the range of $-40 \sim 74$ MeV and $K_{\rm sym}$ in the range of $-460 \sim -270$ MeV. One can see from the above analysis that the range of the density dependence of the symmetry energy is largely reduced as soon as the data with one specific method are concerned. However, if one consider all available data from different methods we find the uncertainties of L and $K_{\rm sym}$ are still very large. However, the calculation results with all available Skyrme interactions around the data obtained with antiprotonic atom roughly form a plateau. This means that the data for neutron skin thicknesses of ^{124}Sn and ^{208}Pb obtained with antiprotonic atom method seem to be better described by more Skyrme interactions. We find that those can reproduce the data obtained with antiprotonic atom method include SKm*, SKp, SLy series, SKX, SKT1-3, which are widely used in calculations of nuclear structure and reactions. Furthermore, concerning the new data of neutron skin thicknesses of isotopes of Sn and ^{208}Pb with SDR(SDR2) method,[5] it seems that the same experimental method provides rather incompatible information of the symmetry energy. For the Sn case the data suggest a very stiff symmetry energy while for the Pb case the data suggest a soft symmetry energy. The reason probably is due to the model dependence of the analysis method. Therefore, it seems to us that a model independent analysis method for extracting the neutron skin thickness is especially important.

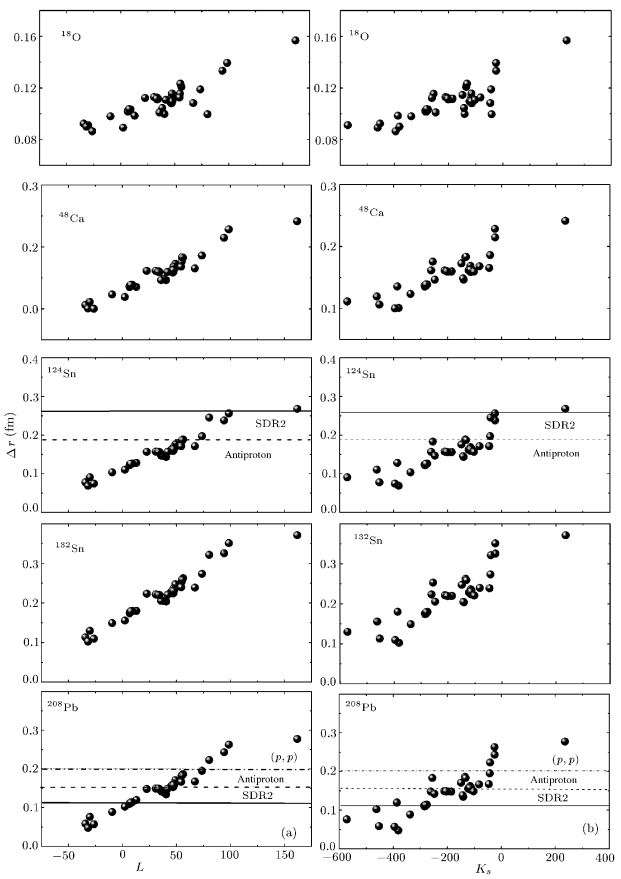

Fig. 4. The neutron skin thicknesses of ^{18}O, ^{48}Ca, ^{124}Sn, ^{132}Sn and ^{208}Pb as a function of (a) L and (b) $K_{\rm sym}$, respectively.

In summary, in this letter the neutron skin thicknesses of even-even Sn isotopes and ^{208}Pb are calculated with 45 Skyrme interactions available up to now and compared with the data obtained with various methods. The calculation results show that the neutron skin thickness increase with the stiffness of the symmetry energy and the data obtained with antiprotonic atom method can be better described by more Skyrme interactions. Our study indicates that the model independent analysis method for extracting the neutron skin thickness is especially important for providing accurate information of the density dependence of the symmetry energy of nuclear matter.

Wang thanks the Alexander von Humboldt-Stiftung Foundation for a fellowship.

References

[1] Horowitz C J and Piekarewicz J 2001 *Phys. Rev.* C **64** 062802
[2] Clark B C, Kerr L J and Hama S 2003 *Phys. Rev.* C **67** 054605
[3] Karataglidis S, Amos K, Brown B A and Deb P K 2002 *Phys. Rev.* C **65** 044306
[4] Alonso D and Sammarruca F 2003 *Phys. Rev.* C **68** 054305
[5] Krasnahorkay A et al 2004 *Nucl. Phys.* A **731** 324
[6] Chen L W, Ko C M and LI B A 2005 *Phys. Rev.* C **72** 064309
[7] Ray L et al 1979 *Phys. Rev.* C **19** 1855
[8] Hoffmann G W et al 1981 *Phys. Rev. Lett.* **47** 1436
[9] Stradubski V E and Hintz N M 1994 *Phys. Rev.* C **49** 2118
[10] Trzcinska A et al 2001 *Phys. Rev. Lett.* **87** 82501
[11] Krasnahorkay A et al 1994 *Nucl. Phys.* A **567** 521
[12] Krasznahorkay A et al 1999 *Phys. Rev. Lett.* **82** 3216
[13] Hohenberg P and Kohn W 1964 *Phys. Rev.* B **136** 864
[14] Brack M, Guet C and Hakanson H B 1985 *Phys. Rep.* **123** 275
[15] Bartel J and Bencheikh K 2002 *Eur. Phys. J.* A **14** 179a
[16] Centelles M et al 1990 *Nucl. Phys.* A **510** 397a
[17] Antonov A N et al 2005 *Phys. Rev.* C **72** 044307
[18] Stone J R et al 2003 *Phys. Rev.* C **68** 034324
[19] Brown B A 2000 *Phys. Rev. Lett.*. **85** 5296